

University of Groningen

Beyond the Nernst-limit with dual-gate ZnO ion-sensitive field-effect transistors

Spijkman, M.; Smits, E. C. P.; Cillessen, J. F. M.; Biscarini, F.; Blom, P. W. M.; de Leeuw, D. M.

Published in:
Applied Physics Letters

DOI:
[10.1063/1.3546169](https://doi.org/10.1063/1.3546169)

IMPORTANT NOTE: You are advised to consult the publisher's version (publisher's PDF) if you wish to cite from it. Please check the document version below.

Document Version
Publisher's PDF, also known as Version of record

Publication date:
2011

[Link to publication in University of Groningen/UMCG research database](#)

Citation for published version (APA):

Spijkman, M., Smits, E. C. P., Cillessen, J. F. M., Biscarini, F., Blom, P. W. M., & de Leeuw, D. M. (2011). Beyond the Nernst-limit with dual-gate ZnO ion-sensitive field-effect transistors. *Applied Physics Letters*, 98(4), 043502-1-043502-3. [043502]. <https://doi.org/10.1063/1.3546169>

Copyright

Other than for strictly personal use, it is not permitted to download or to forward/distribute the text or part of it without the consent of the author(s) and/or copyright holder(s), unless the work is under an open content license (like Creative Commons).

The publication may also be distributed here under the terms of Article 25fa of the Dutch Copyright Act, indicated by the "Taverne" license. More information can be found on the University of Groningen website: <https://www.rug.nl/library/open-access/self-archiving-pure/taverne-amendment>.

Take-down policy

If you believe that this document breaches copyright please contact us providing details, and we will remove access to the work immediately and investigate your claim.

Downloaded from the University of Groningen/UMCG research database (Pure): <http://www.rug.nl/research/portal>. For technical reasons the number of authors shown on this cover page is limited to 10 maximum.

Beyond the Nernst-limit with dual-gate ZnO ion-sensitive field-effect transistors

M. Spijkman,^{1,2,a)} E. C. P. Smits,³ J. F. M. Cillessen,¹ F. Biscarini,⁴ P. W. M. Blom,^{2,3} and D. M. de Leeuw^{1,2}

¹Philips Research Laboratories, High Tech Campus 4, 5656 AE Eindhoven, The Netherlands

²Molecular Electronics, Zernike Institute of Advanced Materials, University of Groningen, Nijenborgh 4, 9747 AG Groningen, The Netherlands

³Holst Centre/TNO, High Tech Campus 34, 5656 AE Eindhoven, The Netherlands

⁴CNR, Institute for the Study of Nanostructured Materials, Via Gobetti 101, I-40129 Bologna, Italy

(Received 30 November 2010; accepted 3 January 2011; published online 24 January 2011)

The sensitivity of conventional ion-sensitive field-effect transistors (ISFETs) is limited to 59 mV/pH, which is the maximum detectable change in electrochemical potential according to the Nernst equation. Here we demonstrate a transducer based on a ZnO dual-gate field-effect transistor that breaches this boundary. To enhance the response to the pH of the electrolyte, a self-assembled monolayer has been used as a top gate dielectric. The sensitivity scales linearly with the ratio between the top and bottom gate capacitances. The sensitivity of our ZnO ISFET of 22 mV/pH is enhanced by more than two orders of magnitude up to 2.25 V/pH. © 2011 American Institute of Physics. [doi:10.1063/1.3546169]

Ion-sensitive field-effect transistors (ISFETs) were first reported 40 years ago.¹ As schematically shown in Fig. 1, ISFETs are based on standard metal-oxide semiconductor field-effect transistors, where the silicon gate electrode has been replaced by an electrolyte grounded with a reference electrode. Ionic interactions at the interface between the SiO₂ gate dielectric and the electrolyte cause a change in the surface potential Ψ_0 . This change in surface potential is detected as a change in threshold voltage V_{th} as $\Delta V_{th} = -\Delta\Psi_0$.² The interface can be modified by applying an ion-selective membrane to make the ISFET selective to specific target molecules.³ ISFETs then allow for label-free detection of ions in solution, negating the need to label the target molecules in a time-consuming polymerase chain reaction.⁴ The small device size allows for easy integration with microfluidics for lab-on-a-chip applications.⁵

The sensitivity of ISFETs has been optimized for pH detection. The proton activity at the interface is related to the surface potential Ψ_0 by the Nernst equation as

$$\Psi_0 = \frac{k_B T}{q} \ln \frac{aH_{bulk}^+}{aH_{surface}^+}, \quad (1)$$

where k_B is the Boltzmann constant, q is the elementary charge, and the symbol a denotes the proton activities in the bulk electrolyte and at the gate dielectric-electrolyte interface. The surface potential can be related to the pH. A detailed analysis has been given by Bergveld,^{2,3} leading to

$$\frac{\delta\Psi_0}{\delta pH} = -2.3 \frac{k_B T}{q} \alpha, \quad (2)$$

where α is a dimensionless parameter, the so-called proton buffer capacity that varies between 0 and 1 and which is a measure for the proton activity of the interface. If α is 1, the ISFET has a so-called Nernstian sensitivity of 59 mV/pH at 25 °C, which is also the maximum achievable sensitivity. In

practice, the value of α is smaller than unity. For SiO₂, α is typically 0.5² and slightly higher values have been reported for more reactive oxides, such as tantalum oxide and erbium oxide.⁶

To improve the sensitivity beyond the Nernstian response, we changed the layout of the ISFET by adding a second gate.^{7–10} A schematic layout of the resulting dual-gate transducer is shown in Fig. 1. The current depends on both the bias on the bottom gate and the surface potential at the gate dielectric-electrolyte interface. It has been shown that a change in the surface potential leads to a shift of the threshold voltage by¹¹

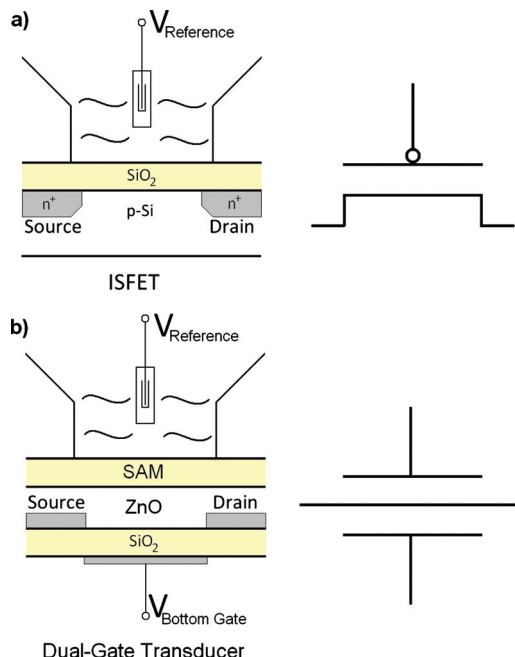


FIG. 1. (Color) Schematic representation of (a) a conventional ISFET and (b) a dual-gate transducer and their corresponding electrical schematics.

^{a)}Electronic mail: mark-jan.spijkman@philips.com.

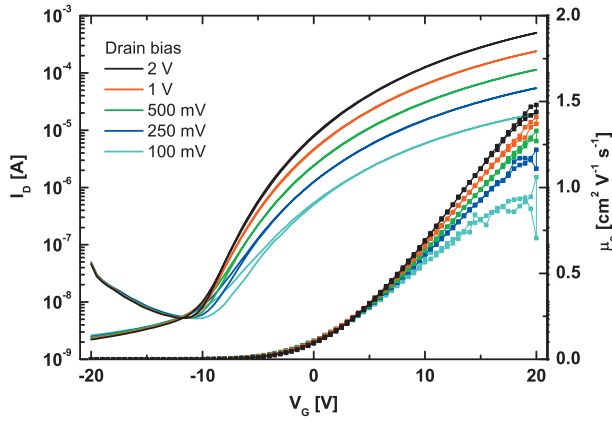


FIG. 2. (Color) Transfer curves of a ZnO transistor for five different drain biases between 100 mV and 2 V. The channel length and width are 10 and 10 000 μm , respectively. Hysteresis is absent, the switch-on voltage is about -10 V, and the linear mobility is about $1 \text{ cm}^2 \text{ V}^{-1} \text{ s}^{-1}$.

$$\Delta V_{\text{th}} = -\frac{C_{\text{top}}}{C_{\text{bottom}}} \Delta \Psi_0. \quad (3)$$

In comparison with a regular ISFET, the change in threshold voltage is modified by the capacitive coupling $C_{\text{top}}/C_{\text{bottom}}$. Dual-gate ISFETs with a capacitive coupling of a factor of 2 have been reported.¹¹ The enhancement was limited due to the use of a relatively thick top gate dielectric. To increase the coupling, a larger top capacitance is required. Here we use a self-assembled monolayer (SAM) as the top dielectric. The bottom capacitance is varied by using different thicknesses of the SiO_2 bottom gate dielectric. Here we determine the response of the dual-gate transducer as a function of the capacitive coupling and we show that the sensitivity can be enhanced by orders of magnitude.

The sensors were fabricated on thermally oxidized n^{++} doped Si as the bottom gate dielectric. We used wafers of various SiO_2 thicknesses. Au source and drain contacts were defined by standard photolithography on a Ti adhesion layer. The n -type semiconductor ZnO semiconductor was deposited on these structured substrates by pulsed laser deposition (PLD).¹² ArF ablation (193 nm, 15 ns) was carried out from high-density ZnO targets that were prepared from ZnO powder. We used high-purity fiber-grade Ultrex ZnO (J.T. Baker, Philipsburg, NJ), which was pressed and subsequently sintered at 1300°C in air. The PLD off-axis geometry was used in order to increase the area of uniform thickness of the deposited films. The layer thickness is about 20 nm. Typical transfer curves for drain biases ranging from 100 mV to 2 V of the resulting ZnO transistor are presented in Fig. 2. Hysteresis is absent, the switch-on voltage is about -10 V, and the linear mobility increase with gate bias to about $1 \text{ cm}^2 \text{ V}^{-1} \text{ s}^{-1}$. The transfer curve for a 100 mV drain bias shows that there is negligible contact resistance.

To realize a large top gate capacitance, we applied a self-assembled monolayer of octadecylphosphonic acid¹³ on top of the semiconducting ZnO. Prior to applying the SAM, the surface is cleaned in O_2 plasma, after which the SAM was applied from a 3 mM ethanol solution. The SAM passivates the ZnO. Therefore, the electrolyte can be applied without affecting the semiconducting channel between source and drain.

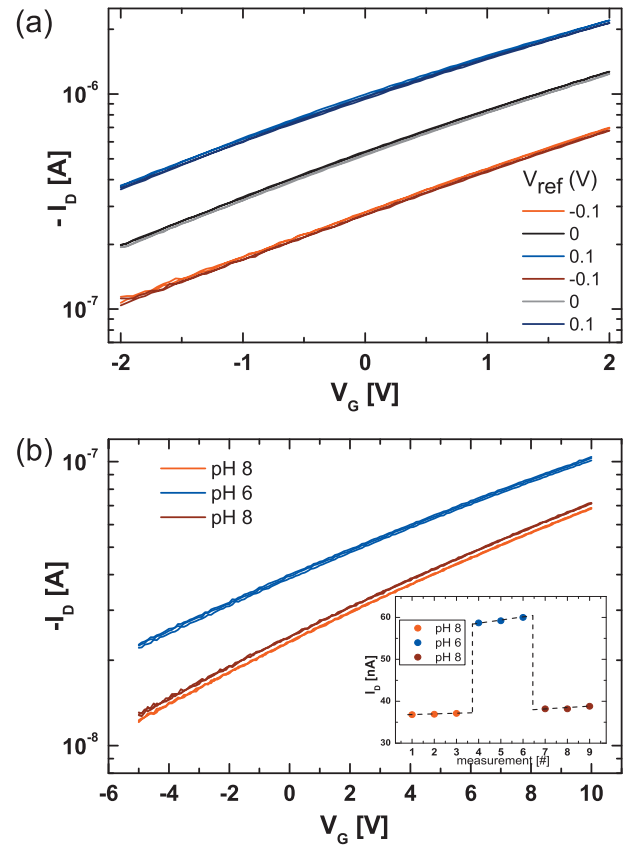


FIG. 3. (Color) Expanded parts of the transfer curves. The drain bias is set at 0.5 V to suppress parasitic Faradaic leakage currents. (a) Transfer curves as a function of the externally applied bias on the Calomel reference electrode to determine the capacitive coupling. (b) Transfer curves measured in buffered electrolyte solutions with pH 6 and 8 and a grounded reference electrode. The inset shows the measurement sequence and the drain current at a gate bias of 4 V. The measurements are reproducible; for a fixed pH , the currents are the same.

The potential of the electrolyte V_{ref} is set by a KCl buffered Ag/AgCl reference electrode. To determine the capacitive coupling, transfer curves were measured as a function of an externally applied bias on the reference electrode. The current as a function of the bottom gate bias is presented in Fig. 3(a). To suppress parasitic Faradaic leakage currents, the drain bias was set at 0.5 V. The transfer curves shift as a function of the bias on the reference electrode. This shift is due to a change in the threshold voltage and can be determined at constant current. The capacitive coupling is then the ratio between ΔV_{th} and ΔV_{ref} . The value extracted from Fig. 3(a) is about 18. The thickness of the bottom SiO_2 gate dielectric of 200 nm yields a bottom gate capacitance of 17 nF/cm^2 . From the capacitive coupling, we extract a value of 300 nF/cm^2 for the top gate capacitance. This capacitance corresponds to an effective dielectric thickness of approximately 8 nm. The effective thickness is larger than the actual SAM-molecule length of about 2 nm. This suggests that the passivated top layer of the ZnO acts as an insulator and contributes to the top capacitance. The origin could be the passivation procedure that might lead to a minor stoichiometry change of the surface layer.

To measure the sensitivity of the transducer toward the pH of the electrolyte, its surface was covered with different pH buffer solutions. The reference electrode was grounded. The current in the linear regime as a function of the bottom

gate bias is presented in Fig. 3(b). Here, the bottom gate dielectric is a 1.2 μm SiO_2 layer. The measurement sequence is shown in the inset. First, the transfer curve was measured three times for pH of 8. Then, a new solution with a pH of 6 was applied and the transfer curves were measured three times. The procedure was then repeated for a pH of 8. The inset shows the current at a gate bias of 4 V. The measurements are reproducible; for a fixed pH , the currents are the same. Figure 3(b) shows that the transfer curve shifts as a function of pH . This shift is due to a change in threshold voltage and can be determined at constant current. Figure 3(b) shows that for a difference in pH of 2, the threshold voltage shifts 4.5 V, yielding a sensitivity of 2.25 V/ pH , which is orders of magnitude larger than the Nernstian response of 59 mV/ pH .

From these measurements, we can derive the proton buffer capacity α . The capacitive coupling of this 1.2 μm thick device was measured to be 110. Hence, corrected for the capacitive coupling, the surface potential Ψ_0 shifts with 22 mV/ pH . This yields a value for α of about 0.4, in good agreement with reported values of about 0.5.

To demonstrate that the sensitivity of the transducer depends on the capacitive coupling, we varied the thickness of the bottom SiO_2 gate dielectric. For transducers with a thickness of 200, 600, and 1200 nm, the capacitive coupling was determined. Transfer curves for each transducer were measured as a function of pH of the electrolyte. The extracted sensitivity is presented in Fig. 4 as a function of the capacitive coupling. Each data point is averaged over about 10 devices. A straight line is obtained in good agreement with Eq. (3). The slope corresponds to a value of α of 0.4 as derived above.

In summary, we have demonstrated a transducer based on a ZnO dual-gate field-effect transistor in which the electrolyte with reference electrode acts as the top gate. To enhance the response to the pH , a SAM has been used as a top gate dielectric. We have shown that the sensitivity scales linearly with the ratio between the top and bottom gate capacitances. The achieved sensitivity of 2.25 V/ pH is orders of magnitude larger than the Nernstian response of 59 mV/ pH . Reliable measurements of, for instance, DNA hybridization and protein interactions might be within reach. For instance, the change in surface potential upon DNA hybridization is typically only tens of millivolts, which hampers the detection with conventional ISFETs. With a dual-gate transducer, the changes can be enhanced to the order of volts.

We gratefully acknowledge P. A. van Hal for fruitful discussions and T. C. T. Geuns from MiPlaza, Eindhoven for

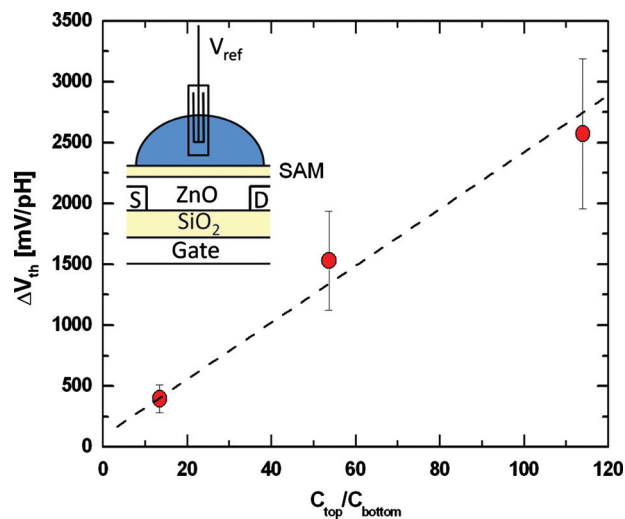


FIG. 4. (Color) The sensitivity of dual-gate transducers in mV/ pH as a function of the capacitive coupling: the ratio between the top and bottom gate capacitances. The data points correspond to bottom gate dielectrics of (from left to right) 200, 600, and 1200 nm SiO_2 . Each data point is averaged over about ten devices. The inset shows the device layout.

technical assistance. We also acknowledge financial support from the Dutch Polymer Institute, project 624 and the European project ONE-P, Grant No. 212311.

¹P. Bergveld, *IEEE Trans. Biomed. Eng.* **BME-17**, 70 (1970).

²P. Bergveld, presented at the IEEE Sensor Conference, Toronto, Canada, 2003.

³G. A. J. Besselink, R. B. M. Schasfoort, and P. Bergveld, *Biosens. Bioelectron.* **18**, 1109 (2003).

⁴K. S. Song, G. J. Zhang, Y. Nakamura, K. Furukawa, T. Hiraki, J. H. Yang, T. Funatsu, I. Ohdomari, and H. Kawarada, *Phys. Rev. E* **74**, 041919 (2006).

⁵D. Goncalves, D. M. F. Prazeres, V. Chu, and J. P. Conde, *Biosens. Bioelectron.* **24**, 545 (2008).

⁶T. M. Pan, J. C. Lin, M. H. Wu, and C. S. Lai, *Sens. Actuators B* **138**, 619 (2009).

⁷G. H. Gelinck, E. van Veenendaal, and R. Coehoorn, *Appl. Phys. Lett.* **87**, 073508 (2005).

⁸S. Iba, T. Sekitani, Y. Kato, T. Someya, H. Kawaguchi, M. Takamiya, T. Sakurai, and S. Takagi, *Appl. Phys. Lett.* **87**, 023509 (2005).

⁹F. Maddalena, M. Spijkman, J. J. Brondijk, P. Fonteijn, F. Brouwer, J. C. Hummelen, D. M. de Leeuw, P. W. M. Blom, and B. de Boer, *Org. Electron.* **9**, 839 (2008).

¹⁰M. Spijkman, E. C. P. Smits, P. W. M. Blom, D. M. de Leeuw, Y. B. Saint Come, S. Setayesh, and E. Cantatore, *Appl. Phys. Lett.* **92**, 143304 (2008).

¹¹M. Spijkman, J. J. Brondijk, T. C. T. Geuns, E. C. P. Smits, T. Cramer, F. Zerbetto, P. Stoliar, F. Biscarini, P. W. M. Blom, and D. M. de Leeuw, *Adv. Funct. Mater.* **20**, 898 (2010).

¹²C. J. Kao, Y. W. Kwon, Y. W. Heo, D. P. Norton, S. J. Pearton, F. Ren, and G. C. Chi, *J. Vac. Sci. Technol. B* **23**, 1024 (2005).

¹³K. Fukuda, T. Hamamoto, T. Yokota, T. Sekitani, U. Zschieschang, H. Klauk, and T. Someya, *Appl. Phys. Lett.* **95**, 203301 (2009).